Characterization of the microstructure of tin-silver lead free solder

Tamás Hurtony[1, a], Alex Szakál[2], László Almásy[2], Adél Len[2,4], Sándor Kugler[3], Attila Bonyár[1], Péter Gordon[1]

[1]Department of Electronics Technology, Budapest University of Technology and Economics, Egry József utca 18. Budapest, H-1111, Hungary

[2]Neutron Spectroscopy Department, Wigner Research Centre for Physics, Budapest

[3]Department of Theoretical Physics, Budapest University of Technology and Economics,

[4]Faculty of Engineering and Information Technology, University of Pécs, Hungary

[a]hurtony@ett.bme.hu

Keywords: A. intermetallics; B. rapid-solidification, quenching; C. microstructure; D. electrochemical impedance spectroscopy

Abstract: Reliability and lifetime are the two most relevant design considerations in the production of safety critical assemblies. For example in a modern automobile dozens of electronic assemblies are integrated in which thousands of solder joints are mounting the electronic components to the printed circuit boards. There exists no standardised and universal observation method for characterising the fine microstructure of such solder joints. Previously we have developed a new method for the quantitative characterization of lead-free solder alloys and in present study the validity of the proposed method is demonstrated. Microstructure of Sn-3.5Ag lead free solder alloy was investigated by electrochemical impedance spectroscopy. Solder samples were solidified with different cooling rates in order to induce differences in the microstructure. Microstructure of the ingots was revealed by selective electrochemical etching. Electrochemical impedance spectra (EIS) were measured before and after the selective etching process. The complex impedance spectra contain information about microstructure of the solder alloys. Comparison and modelling of two EIS spectra allowed obtaining a characteristic parameter of surface structure of the etched specimens. The EIS measurements were complemented with small angle neutron scattering measurements and scanning electron microscopy, in order to correlate the EIS parameter with the magnitude of the interface of the β-Sn and Ag_3Sn phases.

1. Introduction

Lead, being one of the most hazardous substances, has been banned from the electronic industry due to environmental considerations. This initiative has led to the development of new lead free solders for electronic applications[1-5]. All of these solders are Sn based materials with some minor composing elements[6-7]. Nowadays, excellent lead free solder alloys are available on the market, which satisfy the rigorous technical and operational requirements. SnAg (SA) and SnAgCu (SAC) alloys are considered to be the best substitutions for lead containing solders. In these solders Sn-rich dendritic/grainy matrix is formed, and an eutectic mixture of a Sn-rich phase and intermetallic Ag_3Sn particles are located in the interdendritic regions. The fine microstructure of Sn grains and intermetallic compounds (IMC) may be formed differently in function of soldering parameters. Since the macroscopic properties of the solder joints are largely determined by the microstructure, its characterization is a current research topic.

During the lifetime of electrical assemblies the physical parameters of solder joint may change because of environmental effects. One of the most important processes that influences the solder

joint, is the corrosion. This is the reason why the corrosion properties of any solder alloy are in the centre of interest [8-13]. For revealing corrosion properties of the lead free solder alloys, electrochemical methods are usually applied. Osório et al. applied different electrochemical measurements in order to find the correlation between microstructure and corrosion properties of solder alloys [8-10]. The electrochemical corrosion behaviour of Sn–Cu alloy samples was evaluated by electrochemical impedance spectroscopy (EIS) combined with potentiodynamic polarization. According to their results, the impedance response of different samples showed correlation with the microstructure. Independently from the measured electrochemical impedance spectra the examined Sn–Cu solder alloy samples had similar electrochemical corrosion properties, however this was not the case for the electrochemical corrosion behaviour of a Sn–Ag solder alloy. The directionally solidified solder samples inherited different microstructure morphologies, which were evaluated also by EIS. For higher cooling rates finer dendritic arrays and mixture of spheroids and fiber-like Ag_3Sn particles were found, which resulted in better corrosion resistance. The EIS measurement results of Osório et al. were in good correlation with their metallographic observations. Their method however is valid only for directionally solidified samples, and it cannot be used to study solder samples of industrial origin. Furthermore, they applied a selective chemical reagent to reveal the microstructure of their samples, but the level of selectivity could not be guaranteed due to the endothermic nature of the reaction. These limitations can be overcome by the improved characterization method proposed in the present work.

Conventional metallographic observation methods e.g. cross sectioning, provide only a restricted view on the structure of the solder joint. Our novel, recently published method of selective electrochemical etching [14-15], reveals the intermetallic structure of bulk solder and opens a new perspective in solder joint research. Due to the high selectivity of etching, the fine structure of intermetallic compounds is only slightly changed, therefore the original solder structure is revealed.

Previously we found that varying the technological processing conditions - for example the cooling rates - different solder microstructures developed[15]. The utility for qualitatively characterize the microstructure is already introduced and in the present study we propose an industrially applicable method, suited for quantitative characterization of different microstructures.

EIS is very sensitive to the geometry of the working electrodes[16], therefore it was successfully utilized to characterize the roughness of surfaces[17] and even to determine the pore size and shape in the case of porous electrodes[18-20]. Electrochemical etching forms complex surface determined by the microstructure of samples depending on the etching time. While there is no unequivocal relation between EIS characteristics and microstructure, it is safe to presume that the EIS response curves change in a continuous manner upon the variation of a certain parameter of the microstructure, or of the process in which the microstructure is formed. Determination of this relation would allow the usage of the EIS for quantitative characterization of the alloys microstructure.

For this purpose a series of casted solder alloys was prepared by varying the cooling rate and the EIS spectra measured before and after the etching process were compared. The electrochemical behaviour of the samples correlates with the processing parameters and this relation can be used to construct an indicator describing the microstructure.

2. Materials and Methods

2.1 Sample preparation

A commercial, industrial grade solder alloy (ALPHA Vaculoy) of material composition Sn 96%, Ag 3.5% and Cu< 0.05% was used. The solder paste was heated up to 260°C in a thermo resistant test tube in order to separate the metallic and non-metallic phases of the paste. After solidification of the solder ingot, the major part of the still liquid flux was removed and the ingots were grinded and weighed (32 g).

The solder ingots were molten again in a hot air reflow rework station and heated up to the temperature of 260°C. Molten sample was immersed into a defined volume of tempered Galden liquid. After solidification of the solder, disc shaped samples were cut from the ingot for further analysis (see Fig. 1.). Temperature of the solder was monitored with a thermocouple sensor connected to a data logger.

The sliced solder ingots were cold contacted with a measuring wire and they were embedded into a two component acrylic resin. The samples were rasped in a way that the size of their surfaces at the cross sectioning plane was approximately the same. The surface ratios of different samples can be seen in Table 1. The surface of the samples was finished with diamond suspension polishing.

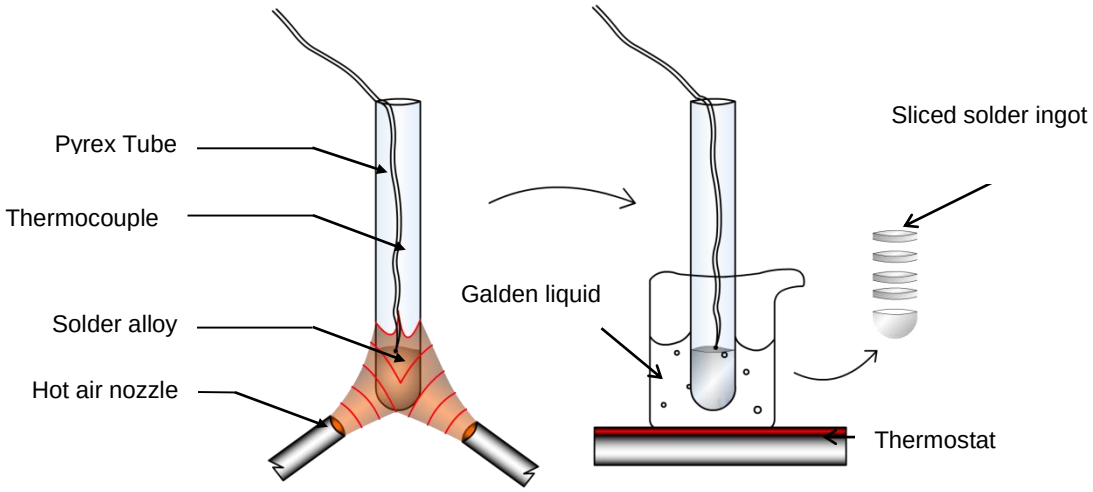

Fig. 1. During the preparation, the samples were heated in a cylindrical symmetric test tube with hot air rework station. The molten solder was immersed into a temperature stabilised pot of Galden liquid.

Table 1. Geometrical properties of the samples

sample ID	S040	S080	S120	S160	S200
Area, mm^2	8.25	7.51	9.49	7.76	7.18
Surface ratio* A_{actual}/A_{S040}	1.00	0.91	1.15	0.94	0.87
Specific surface* $A_{actual}/L_{perimmeter}$	134.8	126.2	152.9	137.5	139.8
Dendrite arm spacing, µm	50±6	62±9	82±13	64±15	112±23
Quenching liquid temperature °C	40	80	120	160	200
Cooling Rate °C/s	-6.6	-3.9	-2.0	-1.2	-0.3

* A_{actual} is the surface of the denoted samples; $L_{perimmeter}$ the length of the circumference of the samples in the sectioning plane.

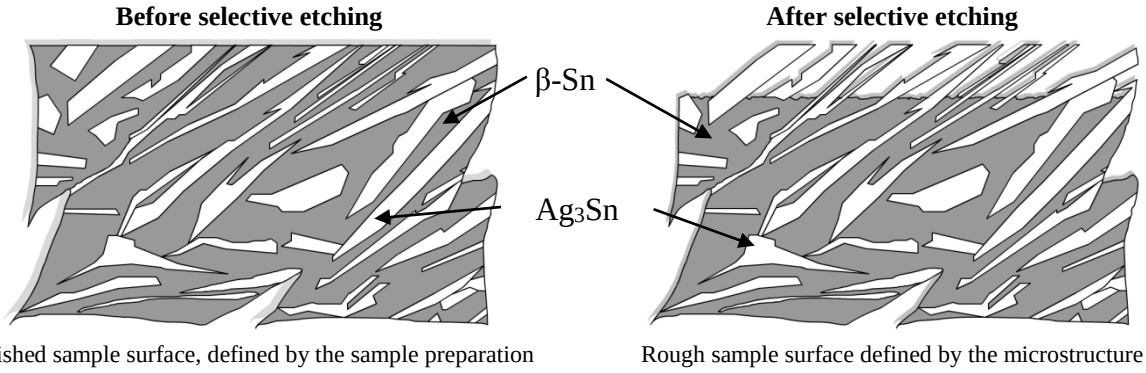

Fig. 2. Before the selective etching process the surface of the work electrode was defined by the polished flat surface. After the selective removal of tin phases the surface of the work electrode is defined by the revealed microstructure of the solder ingot

Embedded and sectioned samples were placed in an electrochemical cell in which the selective etching and also the electrochemical measurements were performed.

2.2 Electrochemical methods

The electrochemical measurement of the samples consisted of three major steps. 1) Reference EIS measurement on the polished samples in in 0.5 M NaCl solution; 2) β-Sn phase removal with selective electrochemical etching in 1 V/V% H_2SO_4 electrolyte; 3) EIS measurement on the etched samples, again in 0.5 M NaCl solution. These measurements were done in a standard three electrode measurement cell configuration, with the samples connected as working electrodes against a stainless steel basin counter electrode and saturated calomel (SCE) reference electrode with a Voltalab PGZ 301 potentiostat. During the measurements the samples were placed to a custom-made electrochemical cell-holder, fixed at 12 mm from the bottom of the stainless steel basin acting as the counter electrode. Only the electrolytes were changed between the three main measurement steps.

The selective removal of the β-Sn phase is possible due to the distinct redox potentials of the β-Sn and Ag_3Sn phases in the applied 1 V/V% H_2SO_4 electrolyte. The etching was done in chrono-amperometry mode, where a fixed DV potential of -350 mV vs. SCE was applied for a given time and the resulting current was monitored. The etching time was chosen to be proportional to the surface area of samples and varied between 120-160 s (see the surface ratios in Table 1). The applied DC potential only etches the β-Sn phase (based on eq. 1), while it is not enough to remove the Ag_3Sn intermetallic compounds, which are hence left intact (Fig 2.).

$$Sn(s) + H_2SO_4(aq) = SnSO_4(aq) + H_2(g) \quad (1)$$

During EIS a small amplitude alternating voltage (in our case a 10 mV peak-to-peak sine voltage) is applied on the working electrode at a fixed DC bias, and the resulting current is measured in function of the frequency (usually between 1 Hz - 50 kHz). The complex impedance of the system can be calculated from the measured current and the drive voltage and it characterizes the electrochemical behaviour of the cell. To qualitatively and quantitatively evaluate this behaviour various network models can be fitted on the measured impedance spectra, where the network elements represent the physical processes, which take place in the cell, more specifically on the surface of the working electrode. In the absence of Faradic processes (which cause electron flow from or to the working electrode, such as redox interactions) the simplest model which can be applied on the working electrode is a simple capacitor (representing the double layer capacitance,

C_{dl}) which is charged and discharged with the applied alternating voltage. In practice the model is often extended with a serial resistance (representing the Ohmic resistance of the electrode (R_s) and the electrolyte) and a parallel resistance (representing the polarisation resistance of electrode (R_p) or the charge transfer resistance (R_{ct}) for the cases when Faradic processes also occur). To guarantee, that no Faradic charge transfer would take place during our EIS measurements – as a result of the 10 mV AC measurement signal – a negative DC bias of -700 mV vs. SCE was applied, which is around 150 mV lower than the measured open circuit potential (OCP, also named zero current potential, which was around -550 mV vs. SCE). Under these conditions we can presume that the system is free of Faradic currents and that the capacitive part of the impedance is defined by the double layer capacitance (C_{dl}), which is associated with the separation of the charge carriers at the interface of the working electrode surface (eq. 2).

$$Z_c(\omega) = -j(\omega C_{dl})^{-1} \quad (2)$$

However this equation only applies for ideally smooth electrodes. Due to the roughness of the electrodes (or heterogeneities of the surface) a so called "capacitance dispersion" is often observed in function of the drive frequency, which means that the phase shift of the capacitance differs from the ideal -90°. To express this phenomenon the double layer capacitance is usually replaced with a so called constant phase element (CPE) in the applied model, and the capacitive part of the impedance is modified as eq. 3.

$$Z_c(\omega)^{-1} = T(j\omega)^{\alpha} \quad (3)$$

T is the CPE coefficient [Fcm^{-2}], which resembles the capacitance of the electrode. α is the CPE exponent, which in practice ranges between 1 (pure capacitance, ideally smooth surface) and 0.5 (porous surface). Since the capacitance of the roughened electrode is depending on the surface area, it is possible to measure the latter by obtaining T through fitting a CPE on the measured EIS spectra. Comparison of the EIS spectra before and after etching and discussion of their behaviour is presented in the Results section. All measurements were carried out at laboratory ambient temperature.

2.3 Scaning Electron Microscopy (SEM) measurements

Microstructure of the samples was evaluated by a FEI Inspect S50 Scanning Electron Microscope. Composing elements were identified by energy dispersive spectroscopy. The Ag_3Sn morphology was quantified by measuring the dendrite arm spacing in the SEM micrographs. The applied method is described in detail by Böyük et al. [21].

2.4 Small Angle Neutron Scattering (SANS) measurements

The nanometer length scale structure of the samples was measured by small angle neutron scattering (SANS) at the *Yellow Submarine* instrument operating at Budapest Neutron Centre. Neutrons of wavelength 1.1 nm and sample-detector distance of 5.5 m were used, covering a q range of 0.08 – 0.4 nm^{-1}. The samples were 1cm diameter discs of 1mm thickness cut from the quenched ingots. SANS probes the bulk of the material and therefore the inner structure of the specimen can be measured without applying the selective etching process.

3. Results and discussion

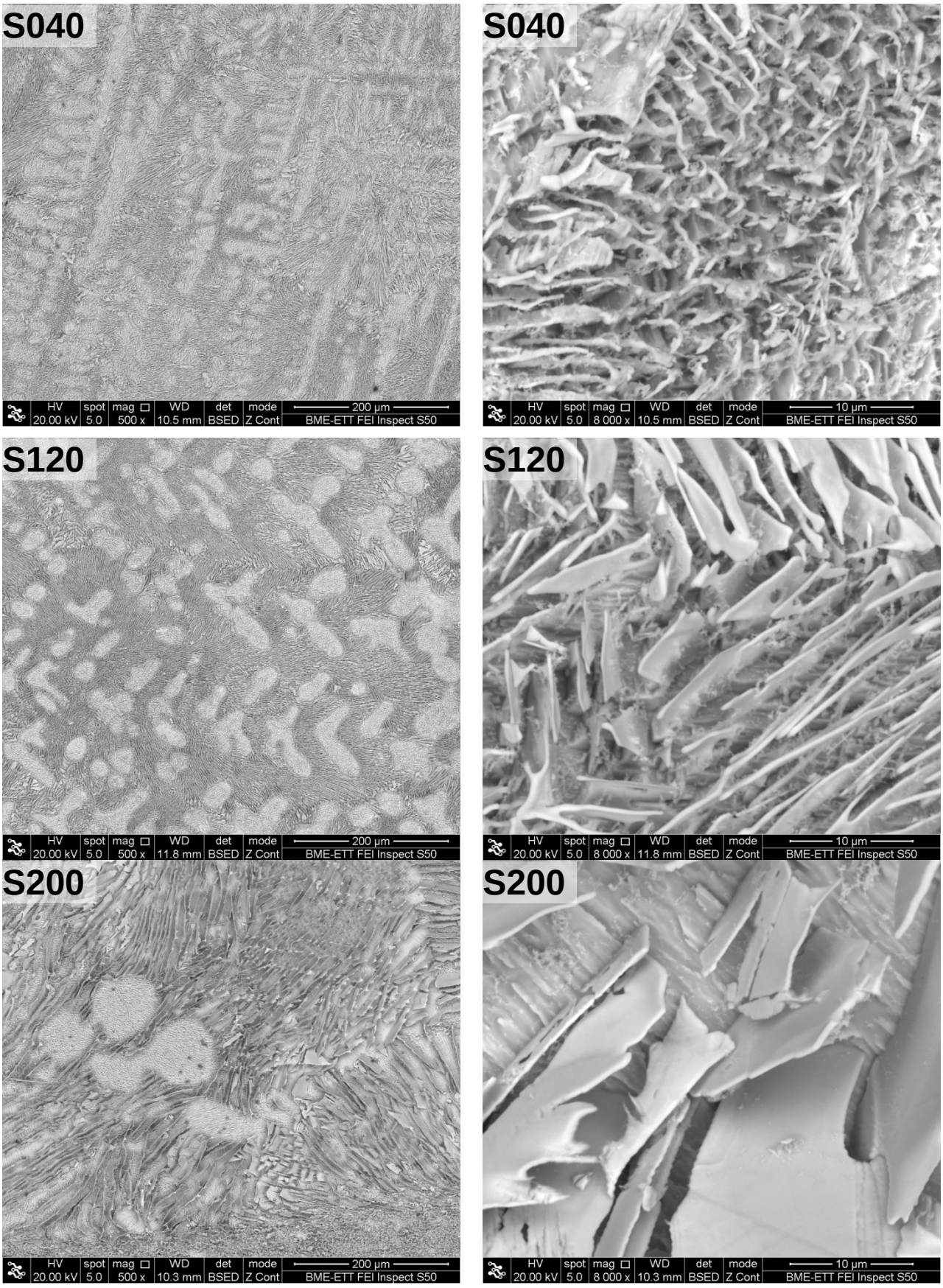

Fig. 3. SEM micrographs of the selectively etched solder samples. The Ag_3Sn intermetallic morphology can adopt spheroid, fibre or plate-like structure. The more rapid the cooling the finer microstructure of IMC array is formed. The average grain size of the dendritic like Sn phases also decreases with increasing cooling rates.

Morphologic analysis of the microstructures was performed with a back scattered electron detector (BSE), because the shading effect of a secondary electron detector might cover structural details of the studied sample (Fig. 3). The IMC morphology is extremely sensitive to any external exposure thus the etching depth had to be limited. The ideal depth of etching is around 60-90 µm. Deeper exposure would carry a risk of damage, which could affect the EIS spectrum.
SEM micrographs for the microstructure evaluation were taken at three different regions of cross sectioning plane, and at least 10 triangles were plotted for calculation of the dendrite arm distances. The results are summarized in the Table 1. In case of S040 sample the fine microstructure of IMC array is mainly composed of fibrous and grainy components. As cooling rate was decreasing, the fine structure transformed to plate like structure, which was in good agreement with other related studies [8-10,21-23].
Due to the reactive nature of the applied electrolyte significant charge transfer was observed in the electrochemical cell during the EIS measurements. This effect was compensated by applying -700 mV offset voltage. The application of offset voltage straightens the measured EIS curves by eliminating the charge transfer process at the surface of electrodes (Fig. 4.)
Spectra taken on the same sample before and after the etching are very different as it can be seen in Fig. 5. Due to selective nature of the etching process, the surface of the work electrode changes drastically, leading to the strong change of the EIS spectrum. Before etching the surface was a polished surface with RA<100 nm, while after exposure the surface was determined by the surface of IMC in the exposed depth.

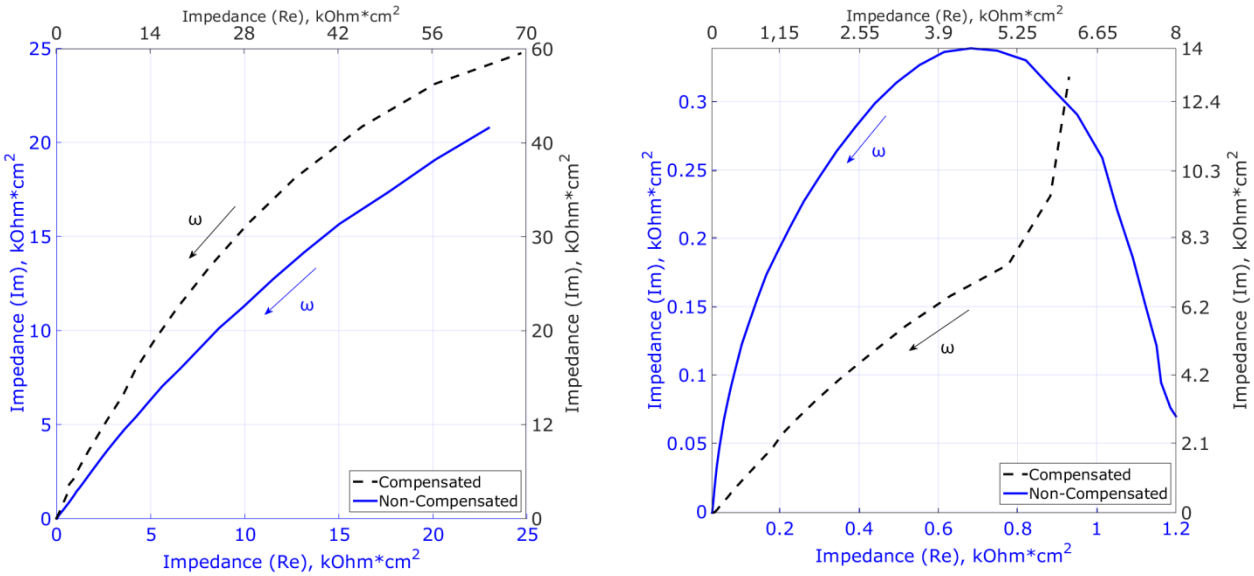

Fig. 4. The before (left) and the after (right) EIS spectra of the Compensated and the Non-Compensated cases. -700 mV offset voltage was applied during the compensation in order to prevent the chemical reaction at the surfaces of the electrodes and to eliminate the charge transfer.

The EIS spectra were analysed by considering the physical processes in the electrochemical reaction and constructing the corresponding equivalent network circuit of the electrochemical system. The free parameters of the model were fitted to the measured data[8-12]. Using the offset voltage, a simpler model of the equivalent network could be applied, consisting of a serial connection of a resistor (R1) and a constant phase element (CPE1). In order to take into account the effect of inhomogeneous field on the surface of the work electrode a polarisation resistance was connected parallel to the CPE1 The fitted polarisation resistances were extremely high, therefore including this parameter did not affect noticeably the CPE1 value [24]. The network parameters of the equivalent circuits of the 'after' spectra alone were not suitable for the microstructure characterisation, since the value of the CPE1 is determined partially by the geometry of the electrochemical cell. Ratio between dominant CPE1 parameter of the 'before' and the

corresponding ‘after’ spectra were calculated in order to eliminate the effect of cell geometry. The impedance ratio of these spectra is shown in Fig. 6. The impedance ratio increased as the temperature of the quenching medium decreased, and showed a clear, nearly linear trend for the studied sample series (Fig. 6).

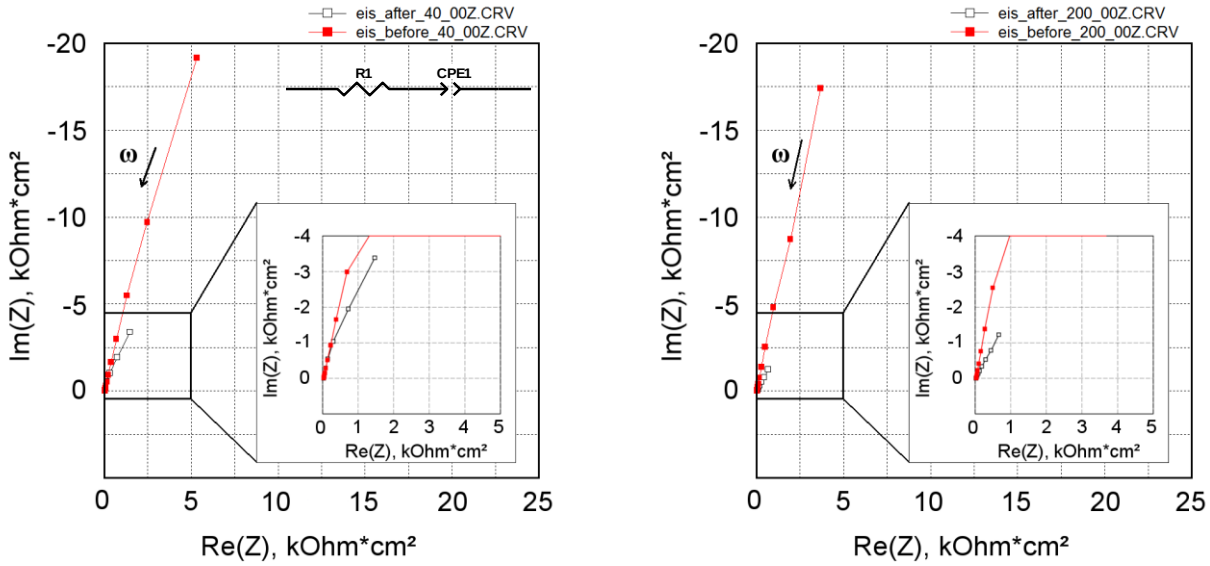

Fig. 5. The measured ‘before’ and ‘after’ EIS spectra of the S040 (left) and S200 (right) samples. The equivalent network circuit which was applied during the evaluation of the spectra can also be seen. The constant phase element (CPE1) is the most dominant component in the serial connection the R1 resistor and CPE1.

Since the impedance change is mainly caused by the revealed microstructure of the solder sample, the ratio of the CPE1 parameters is in a good correlation with the surface of intermetallic phase. The higher the impedance change between the ‘before’ and the ‘after’ spectra, the larger the interface is and indicating that the IMC structure is finer.

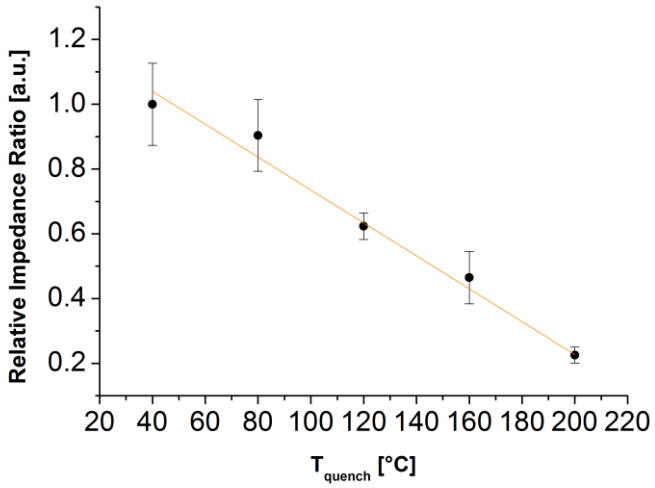

Fig. 6. The ‘before’ / ‘after’ ratio of the dominant CPE1 elements. The ratios are normalized to the ‘before’ / ‘after’ ratio of sample S040.

3.3. Small angle neutron scattering

The samples consisted of interdigitated phases of Sn and Ag_3Sn as it can be seen in SEM micrographs (Fig. 3). For a two phase system with smooth interfaces, the scattering intensity obeys the Porod law, expressed by Equation 4:

$$I(q) = Aq^{-4} + bg \qquad (4)$$

The SANS scattering curves reveal the presence of a sharp interface between phases in the studied size range (50-500 nm) as it follows from the -4 slope of the log I (q) vs. log q graphs (see inset in Fig 7.).

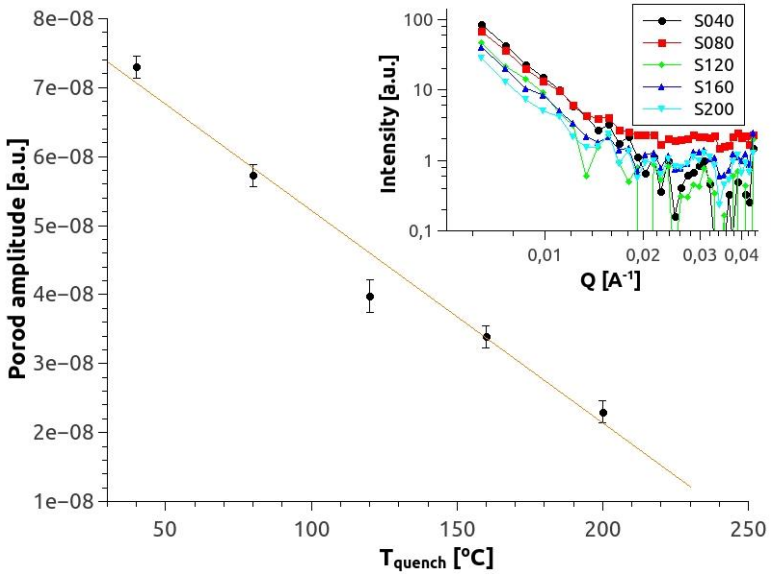

Fig. 7. Amplitude (A) of the fitted Porod equations in function of the cooling liquid temperature (T_{quench}). Inset: the measured SANS scattering curves for the different samples.

The coefficient A in Eq. 4. is proportional to the amount of the interfaces and to the square of contrast between the two phases. Contrast in SANS is defined as the difference in scattering length densities of the neighbouring phases, which is determined by their atomic composition and density. In present case the contrast remains the same for all samples, therefore the coefficient A is proportional to the specific surface in the samples, and it can be used as a measure of the interface of the two phases.
In Fig. 7 the parameter A is plotted in function of T_{quench}. The specific interfaces increase with decreasing the quenching temperature. The surface increase can be explained by that at higher speed of quenching (at lower T_{quench}) the crystal growth process is stopped earlier thus the size of crystallites are smaller. The total amount of Ag_3Sn phase is the same for all samples, since it is determined by the added Ag. Decreasing the crystallite size thus results in increased surface.

The monotonic dependence of the specific surface on quenching temperature for the series of samples is in qualitative agreement with the SEM results, and it correlates linearly with the behaviour of the $CPE1_{before}/CPE1_{after}$ ratio. The proposed method therefore allows to characterize the solder alloy interface in a semi-quantitative way.

3. Summary and conclusions

An electrochemical method for characterising the microstructure of lead free solder alloy is presented in this paper. Sn3.5Ag solder samples were reflowed and quenched in Galden liquid with different temperatures in order to generate different microstructures. The microstructure was revealed with selective electrochemical etching and the electrochemical impedance spectra were measured before and after the etching process in the same electrochemical cell geometry, in order to assess only the structure of the revealed microstructure. The before-after ratios of the dominant constant phase elements (CPE) of the equivalent network circuits serve as a quantitative parameter

characterizing the surfaces of the revealed microstructures. This parameter is shown to be in linear correlation with the amount of interface between the Sn and Ag_3Sn phases as measured by small angle neutron scattering. SEM measurements on the selectively etched surfaces have shown that the microstructure is composed of fibre grain and plate-like Ag_3Sn intermetallic compounds in the Sn matrix (Fig. 3). Higher cooling rate yields finer structure. The relative occurrence of fibre and grainy type structures was larger in samples with higher cooling rate, while at lower cooling rate more plate-like structures formed. The results of SANS and SEM measurements confirmed the applicability of the combination of the new selective etching and EIS with the proposed evaluation method to characterize the lead-free solder alloy microstructure. The proposed method is fully compatible with the commonly used metallographic and stereological observation routine, but it can provide numerical value, which correlates with the surface of the tin-silver intermetallic phase.
The new method is sufficiently fast, precise and cost effective to be applied in an industrial environment for monitoring the microstructure of lead free solder joints and it can also be used in scientific research. Many researches that have been carried out in connection with lead-free solder alloys could be reproduced and supplemented with the proposed method in order to relate the macroscopic properties to the parameters of the microstructure quantitatively.

4. Acknowledgement

The research leading to these results has received funding from the ProProgressio foundation.

5. References

1. S.P. Yu, H.J. Lin, M.H. Hon, Effects of process parameters on the soldering behavior of the eutectic Sn–Zn solder on Cu substrate, J. Mater. Sci. 11, (2000), 461–471.
2. R.A. Islam, Y.C. Chan, W. Jillek, S. Islam, Comparative study of wetting behaviour and mechanical properties (microhardness) of Sn–Zn and Sn–Pb solders, Microelectron. J. 37, (2006), 705–713.
3. E. Çadırlı, U. Böyük, S. Engin, H. Kaya, N. Maraslı, A. Ülgen, Experimental in the Sn–1.2 wt.% Cu alloy, J. Alloys Compd. 486, (2009), 199–206.
4. L.R. Garcia, W.R. Osório, L.C. Peixoto, A. Garcia, Mechanical properties of Sn–Zn lead-free solder alloys based on the microstructure array, Mater. Charact. 61, (2010), 212–220.
5. Y. Jing, G. Sheng, G. Zhao, Influence of rapid solidification on microstructure, thermodynamic characteristic and the mechanical properties of solder/Cu joints of Sn–9Zn alloy, Mater. Des. 52, (2013) , 92–97.
6. Seo SK, Kang SK, Shih DY, Lee HM. An Investigation of Microstructure and Microhardness of Sn-Cu and Sn-Ag Solders as Functions of Alloy Composition and Cooling Rate, J. Electron. Mater. 38(2), (2009), 257–65.
7. E. Bastow, Solder families and how they work. Adv. Mater. Process 2003; 3:26–9.
8. W. R. Osório, E. S. Freitas, J. E. Spinelli, A. Garcia, Electrochemical behavior of a lead-free Sn–Cu solder alloy in NaCl solution, Corros. Sci. 80, (2014), 71–81.
9. W. R. Osório, L. R. Garcia, L. C. Peixoto, A. Garcia, Electrochemical behavior of a lead-free SnAg solder alloy affected by the microstructure array, Mater. Des. 32, (2011) 4763-4772.
10. W. R. Osório, J. E. Spinelli, C. R.M. Afonso, L. C. Peixoto, A. Garcia, Microstructure, corrosion behaviour and microhardness of a directionally solidified Sn–Cu solder alloy by the microstructure array, Electrochim. Acta 56, (2011), 8891– 8899.
11. F. Rosalbino, E. Angelini, G. Zanicchi, R. Carlini, R. Marazza. Electrochemical corrosion study of Sn–3Ag–3Cu solder alloy in NaCl solution, Electrochim. Acta 54/28, (2009), 7231-7235.

12. A. Wierzbicka-Miernik, J. Guspiel, L. Zabdy, Corrosion behavior of lead-free SAC-type solder alloys in liquid media, Arch. Civ. Mech. Eng., 205, (2014), 206–213.
13. B.P. Markhali, R. Naderi, M. Mahdavian, M. Sayebani, S.Y. Arman, Electrochemical impedance spectroscopy and electrochemical noise measurements as tools to evaluate corrosion inhibition of azole compounds on stainless steel in acidic media, Corros. Sci. 75, (2013), 269–279.
14. T. Hurtony, A. Bonyár, P. Gordon, G. Harsányi, „Investigation of intermetallic compounds (IMCs) in electrochemically stripped solder joints with SEM", Microelectron. Reliab. 52, (2012), 1138-1142.
15. T. Hurtony, A. Bonyár, P. Gordon, Microstructure comparison of soldered joints using electrochemical selective etching, Mater. Sci. Forum. 729, (2013), 367-372.
16. C. G. Zoski, Handbook of Electrochemistry, Elsevier, 2006
17. D. Ende, W. Kessler, D. Oelkrug, R. Fuchs Characterization of chromate-phosphate conversion layers on Al-alloys by electrochemical impedance spectroscopy (EIS) and optical measurements, Electrochim. Acta, 38/17, (1993), 2577-2580.
18. R. Jurczakowski, C. Hitz, A. Lasia, Impedance of porous Au based electrodes, J. Electroanal. Chem. 572, (2004), 355–366.
19. D. Gimenez-Romero, J.J. Garcıa-Jareno, F. Vicente, Correlation between the fractal dimension of the electrode surface and the EIS of the zinc anodic dissolution for different kinds of galvanized steel, Electrochem. Commun. 6, (2004), 148–152.
20. A. Lasia, Impedance of Porous Electrodes, ECS Transactions 13, (2008), 1-18.
21. U. Böyük, S. Engin, H. Kaya, N. Maraşlı, Effect of solidification parameters on the microstructure of Sn-3.7Ag-0.9Zn solder, Mater. Charact. 61, (2010), 1260 -1267.
22. U. Böyük, N. Maraşlı, Dependency of eutectic spacings and microhardness on the temperature gradient for directionally solidified Sn–Ag–Cu lead-free solder, Mater. Chem. Phys. 119, (2010), 442–448.
23. L. R. Garcia, W. R. Osório, A. Garcia, The effect of cooling rate on the dendritic spacing and morphology of Ag3Sn intermetallic particles of a SnAg solder alloy, Mater. Des. 32, (2011), 3008–3012.
24. O.E. Barcia, E. D'Elia, I. Frateur, O.R. Mattos, N. Pe, B. Tribollet, Application of the impedance model of de Levie for the characterization of porous electrodes, Electrochim. Acta 47, (2002), 2109-2116.